

Investigation of UCL Tears in Baseball Pitchers

A Major Qualifying Project
Submitted to the Faculty of
Worcester Polytechnic Institute
in partial fulfillment of the requirements for the
Degree of Bachelor of Science
in
Mechanical Engineering
by

Maddie Brennan

Stephen Gallagher

Benedict Kurtze

Paula Sardi

Date: 4/ 25 / 2019

Advisor: Professor Marko Popovic

Co-Advisor: Professor Selçuk Guçeri

Abstract

Tearing of the ulnar collateral ligament (UCL) is one of the most common injuries for baseball pitchers. During a pitch, the UCL experiences high levels of stress between the cocking and acceleration phase due to a valgus moment. Because this stress cannot be directly measured in vivo, a pitching robot with numerous biomimetic features was created to gain a better understanding of these forces during a fastball pitch. This robotic research platform was then used to design a brace that reduces the amount of stress the ligament undergoes, potentially prolonging the play time for athletes. The robotic arm, in the form of a human skeletal replica, featured seven independently, pneumatically actuated Hydro Muscles and a biomimetic UCL. When the brace was used on the robotic arm, the force on the artificial UCL decreased during the pitching phases which validated its effectiveness.

Acknowledgements

The completion of this project would have not been possible without the support of our advisor, Professor Marko Popovic, and our co-advisor, Professor Selçuk Guçeri. We greatly appreciate their constructive feedback, as well as their advice for approaching problems along the way. We also benefited from the equipment and resources in Popovic Labs.

We would also like to thank Shannon M. Moffat, a Robotics Master student in Popovic Labs, who guided us during our project while providing resources and background from previous, relevant projects.

We would like to extend our gratitude towards the Mechanical Engineering Department for their financial support, as well as their educational support. The team was able to use our academic backgrounds and learning from the past four years in approaching this extensive project.

Lastly, we would like to thank the other students working in Popovic Labs this year. We were able to create a support system for the late nights in the lab, and it was beneficial for us to collaborate with like-minded people.

Table of Contents

Abstract	2
Acknowledgements	3
Chapter 1: Introduction	6
Chapter 2: Background	7
2.1 Baseball Pitch	7
2.2 Existing Braces	9
2.3 Ulnar Collateral Ligament	10
2.4 Linear Displacement Sensors	10
2.5 Hydro Muscles	11
Chapter 3: Project Objectives	13
Chapter 4: Methodology	14
4.1 Skeletal Model	14
4.1.1 Hydro Muscles	14
4.1.2 Skeleton	15
4.1.3 Structure	15
4.1.4 Air Tank and Valves	16
4.2 Sensor and Controls	16
4.2.1 Sensors	16
4.2.2 Arduino Mega	17
4.3 Brace Design	17
Chapter 5: Experiments	19
Chapter 6: Results	20
6.1 Comparison of Human and Robotic Arm Pitch	20
Chapter 7: Discussion	24
7.1 Analysis of Robot Kinematics	24
Chapter 8: Conclusion	26
References	27
Appendix A	30
Appendix B	31
Appendix C	33

Table of Figures

Figure 1. Phases of Pitching (Physiopedia contributors, 2019)	8
Figure 2. Compressive Brace (McDavid, 2019)	9
Figure 3. Postoperative Brace (Ortho Depot, 2019)	9
Figure 4. Bauerfeind Elbow Brace (Bauerfeind, 2016)	9
Figure 5. Ulnar Collateral Ligament Bands (LMH Health, 2019).....	10
Figure 6. Strain Gauge (Culler, 2017).....	10
Figure 7. Hall Effect Sensor (Core Electronics, 2013)	11
Figure 8. Stretch Sensor (Sector67, 2019)	11
Figure 9. Hydro Muscle Relaxed and Pressurized (Curran, Colpritt, Sullivan, & Moffat, 2018)	11
Figure 10. Hydromuscle Materials and Construction (Curran et al., 2018).....	14
Figure 11. Arm Model Assembly	16
Figure 12. Sensor Materials and Stretch Sensor Configuration.....	17
Figure 13. Brace Concepts and Final Prototype	18
Figure 14. Early Cocking of Test Pitcher	20
Figure 15. Early Cocking of Robot.....	20
Figure 16. Release Point of Test Pitcher.....	21
Figure 17. Release Point of Robot	21
Figure 18. Change in Resistance Through Time Graph.....	22
Figure 19. Relationship between Force and Change in Resistance Graph	22
Figure 20. Force on the UCL During a Baseball Pitch Graph	23
Figure 21. Brace Prototype Being Worn.....	25

Chapter 1: Introduction

Baseball, also known as America's favorite pastime, has been consistently growing in participation since 1969 (*Participation statistics*.2013). As a result of this growth, the number of injuries has also increased, specifically in young pitchers. Due to the repetitive nature of the throw, tears of the ulnar collateral ligament (UCL) in the elbow are very common in baseball pitchers (OrthoInfo, 2018). The UCL tears since it undergoes high amounts of stress during the late cocking phase of a baseball pitch, which is where external rotation of the shoulder and arm is at its maximum (Weeks & Dines, 2015).

The exact stresses of the UCL during a pitching motion cannot be measured directly, as the ligament is not compatible with in vivo sensors. In general, UCL material properties are very limited since most studies have been done on cadaveric models. Therefore, there is a need for a better understanding of baseball biomechanics and the impact a pitch has on the UCL. This is necessary to learn how to prevent injury, or prolong the playing time of the athlete before the need of a surgical intervention.

The overall goal of this project was to create a brace that will reduce the stresses the UCL undergoes during a baseball pitch, allowing for the aforementioned injury prevention. In order to do so, a testing mechanism was created, using a skeletal arm model, to mimic the movement of a fast ball baseball pitch. Through biomechanical analysis, muscles in the upper arm and shoulder that play a major role in the pitching motion were selected. Hydro Muscles, pneumatic actuators resembling biological muscles, were used to produce a human-like fastball pitch, and leather was used to act as a synthetic UCL, due to its similar material properties. Measurements were then taken on this material using a linear displacement sensor. To test the effectiveness of the brace, the skeletal arm was interfaced with it, and measurements of the synthetic UCL with and without the brace were recorded.

In Chapter 2, the conducted background research is introduced for a better understanding of the project. This includes more knowledge on baseball and baseball biomechanics, existing elbow braces on the market for baseball players, human arm anatomy and UCL properties, and, lastly, background research used for the robotic arm which includes various types of linear displacement sensors, and Hydro Muscles and its applications. Chapter 3 lists the project objectives attained to achieve the goal. Chapter 4 describes the methodology used to create the robot and brace design. Chapter 5 describes the experiments conducted with and without the brace using the robotic arm. Chapter 6 details the results obtained from the experiments. Chapter 7 discusses these results pertaining to the effectiveness of the brace as well as limitations of the project. Lastly, Chapter 8 concludes the project, reiterating the goals and results, as well as addresses improvements and future directions for this project.

Chapter 2: Background

2.1 Baseball Pitch

Originally a gentleman's game, baseball was created in the late 1800's, since then it has grown in popularity exceptionally (History Staff, 2019). Baseball has evolved into a multi-billion dollar business where those who excel, earn millions of dollars to play professionally. These kind of incentives have changed the sport of baseball at the youth level dramatically over the past several decades. Participation of high school players has increased from approximately 360,157 to almost half a million since 1969 (*Participation statistics*.2013).

Unfortunately there is a high physical demand for high school players that are hoping to excel in this sport, which may lead to career altering or ending injuries. Common baseball related injuries include tearing of the rotator cuff or Ulnar Collateral Ligament (UCL). When the UCL tears, players must undergo a UCL reconstructive surgery, commonly known as Tommy John Surgery. This surgery can set players back 8-14 months before they return to their previous level of play (Johns Hopkins Medicine, 2019). The number of UCL surgeries has been surging upward over the past several decades at an alarming rate at the professional and youth levels. In an interview with Dr. Mininder Kocher, Associate Director of the Division of Sports Medicine and Professor of Orthopaedic Surgery at Harvard Medical School, claims that he, alone, performs over 30 Tommy John surgeries on youth athletes every year. But where is this surge coming from?

Research shows that pitching more often, for a longer period of time drastically increases one's risk of injury. For example, when a player pitches competitively for more than 8 months per year, it increases the odds of surgery by five times. Pitching more than 100 competition innings in a year triples the risk of a serious elbow or shoulder injury and with more than 80 pitches in a game the chance of surgery almost quadruples (Fleisig & Andrews, 2012). Opportunities to participate in more games per year was made possible by the creation of organizations such as the Amateur Athletic Union (AAU) and Perfect Game Incorporated. The AAU created a travel baseball league for excelling athletes in 1983 and Perfect Game Incorporated was created in 1995 for youth to be exposed to a college and professional level environment (AAU Baseball, 2019; Perfect Game, 2019). Players who are part of these teams start preparing for their seasons in the early winter months, play on the weekends of the school season, through the summer, and well into the fall. Therefore, pitchers tend to pitch for about 8 months in a calendar year, if not more. This can increase the number games played per calendar year from 20 games to 70 games meaning anywhere from 70-100+ innings are pitched, plus time in the field accumulating on their arms (Johns Hopkins Medicine, 2019).

It's not only the high volume of throwing that has led to the uptick in UCL injuries, but it is also the impulse each individual throw has on the arm. The overhead throwing motion is inherently unnatural for the body to perform, and the average velocity of a fastball baseball has risen in the past few decades from 90 mph to around 92.5 mph as of 2015 (Doran, 2015). While this jump may not seem significant, a 90 mph pitch already is pushing the maximum threshold of the UCL and any further increase can have significant consequences. This speed forces joints into highly torqued positions that they are not naturally intended to be in.

During a pitch the forearm can reach up to 190 degrees of external rotation (Oyama, 2012). This happens during the transition from the cocking phase of a pitch to the acceleration phase. There are six stages to a baseball pitch, windup, early cocking, late cocking, acceleration, deceleration, and follow-through. **Figure 1** below displays each of these stages.

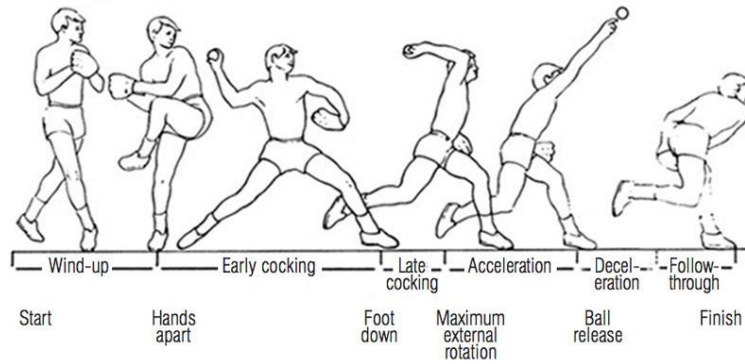


Figure 1. Phases of Pitching (Physiopedia contributors, 2019)

The windup phase is when the pitcher keeps their center of gravity on their back leg, then elevates the lead leg and separates the throwing hand from the glove. The early cocking phase begins when the lead leg reaches maximum height and the standing leg then initiates pelvic rotation and forward tilt. The shoulder then starts to externally rotate through the use of the supraspinatus, infraspinatus, and teres minor, positioning the humeral head on the glenoid. Other muscles, such as the middle trapezius, rhomboid, and levator scapulae move the glenoid in order to provide the humerus with a stable base for rotation. The leading leg that is elevated then lands in line with the stance foot, pointing towards home plate. This foot contact then begins the late cocking phase. During late cocking the arm is flexed, through activation of the biceps muscle, the humerus undergoes abduction and extreme external rotation while the scapula is retracted. There are a number of muscles involved in order to create this large rotation. The teres minor and infraspinatus are two of the main muscles to cause external rotation of the humerus. Scapula retraction is achieved by the contraction of the subscapularis, pectoralis major and latissimus dorsi. The torso continues to rotate and is tilted forward and laterally and the knee of the leading leg begins to extend. The termination of the late cocking phase and the beginning of the acceleration phase is when the shoulder and elbow reach maximum external rotation. The lower half of the body, also known as the trunk, continues to rotate and tilt during acceleration as the knee extends and the hip of the lead leg flexes. This provides a more stable base and increases the angular momentum of the trunk which in turn increases the velocity of the ball. The humerus horizontally adducts and then internally rotates forcefully within 58 milliseconds. In order to create such a quick change of direction, the subscapularis, pectoralis major, and latissimus dorsi reach maximum activity. The serratus anterior also reaches maximum activity to protract the scapula to provide a stable glenoid for the humerus to rotate. The elbow also extends from 90 degrees to 120 degrees by the contraction of the triceps and the ball is released, ending the acceleration phase. In deceleration the arm continues to adduct and internally rotate, and the shoulder soft tissues dissipate the forces caused from the acceleration phase. The teres minor, infraspinatus, and posterior deltoid are responsible for this dissipation. The humeral head is restricted from translation, horizontal adduction, and internal rotation by the highly activated teres minor. Elbow extension and forearm pronation are further decelerated by the biceps and brachialis. Lastly, the follow-through phase is where the body continues to move forward with the arm until motion stops and muscle firing decreases (T Seroyer et al., 2010). When combined with an intent for maximum velocity, these actions occur over milliseconds and focus the energy transferred from the legs, through trunk and arm building up into the elbow just before release creating high forces running through the UCL.

2.2 Existing Braces

Braces aimed toward baseball players that currently exist include postoperative braces or general compression braces for comfort. In terms of braces that are used to help prevent injuries for throwing, there are very few, and more specifically to support the UCL during throwing, virtually none. In a throwing motion the shoulder can rotate at upwards of 7,500 degrees per second and the elbow can rotate at over 2,200 degrees per second (T Seroyer et al., 2010). This puts an incredible amount of stress on the UCL. To limit the high torque effect that occurs in the UCL during the throwing motion, there needs to be a high resistance to force, which is hard to create in a brace that needs such a fluid and high range of motion in such a short time period.

Postoperative braces tend to restrict athletic motion which is not useful for supporting a dynamic pitching movement. Braces needed for rehabilitation possess options of fixed protection, locked articulation, adjustable range of motion, or dynamic and static progression (Fusaro, Orsini, Sforza, Rotini, & Benedetti, 2014). Therefore, these types of braces cannot be used in practice or in games. Braces that are typically used during active play are typically compressive braces. Compressive braces are beneficial to increase blood flow throughout the arm and stabilize muscles which are primarily just for the athletes comfort (Fleet Feet Hartford, 2019). Unfortunately, these braces are typically just a layer of fabric and do not provide any resistance or support needed to prevent injury to the elbow. Typical postoperative braces and compressive braces resemble the braces shown in Figures 2 and 3.



Figure 3. Compressive Brace (McDavid, 2019)



Figure 2. Postoperative Brace (Ortho Depot, 2019)

One brace that is found to be preventative for injuries is the Bauerfeind Elbow Brace. This brace's primary function is to prevent overextension of the elbow at the very end of the throwing motion (Bauerfeind, 2016). Not only is this brace supposedly able to be used preventatively, but it can also be used post operatively for protection. The Bauerfeind brace is shown in Figure 4.



Figure 4. Bauerfeind Elbow Brace (Bauerfeind, 2016)

The research behind this brace claims that during the follow through stage of the pitch, the bones collide together which can cause injury to ligaments after a repeated number of throws. Unfortunately the anterior band of the UCL is not incorporated in resisting extension of the radius and ulna from the humerus, its primary function is to resist transversal stress across the elbow joint. The Bauerfeind Brace provides many promising aspects, but unfortunately the effectiveness has not been clinically proven (Snyder, 2016). This leaves room for the preventative brace market to grow, especially in resisting the valgus forces the elbow is subjected to while throwing.

2.3 Ulnar Collateral Ligament

The ulnar collateral ligament is a bundle of three triangular shaped bands: the posterior, transverse and anterior bands, and is on the inside part of the elbow (Andrews, Dugas, Cain, & Jost, 2012, Labott, Aibinder, Dines, & Camp, 2018). The orientation of each of the sections is shown in Figure 5 below.

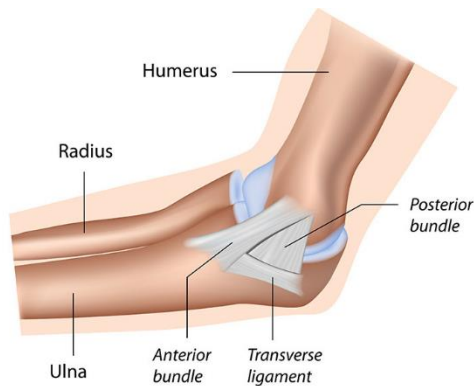


Figure 5. Ulnar Collateral Ligament Bands (LMH Health, 2019)

The anterior band (AB) is known as the longest ligament of the elbow. According to recent studies, the length is between 51.7 to 53.9 mm and the width ranges from 4.0 to 7.6 mm (Labott et al, 2018). It joins the ulna and humerus together resisting valgus stress. Overhead throwing athletes commonly injure their AB due to cyclic loading of valgus stress on the elbow during the cocking and acceleration phases of the throw (Andrews et al, 2012). The injury results in pain, instability, decreased velocity and reduced accuracy during performance (Labott et al, 2018). Usually, it requires surgical intervention for a faster recuperation.

Very little research has been done on the UCL in vivo, most of it has been on cadaveric models. Valgus moment tests have been performed to measure the mechanical material properties but have stated that in vivo UCL's undergo higher stresses during athletic performance. The lack of in vivo tests and measurements has been an obstacle to better the understanding of the biomechanics of the ligament. There is little information about the material properties of the elbow's UCL. Literature claims that human ligament specimens share general material properties. CES Edupack 2018 software defines the Young's Modulus of human ligament to range from 0.08 to 0.3 GPa. The range of the modulus is so large because the properties of ligaments depends on the composition and structure of the specific specimen. This was found when another study demonstrated an even larger Young's Modulus range of 0.05 and 0.45 GPa (Dolan & Drew, 2005)

2.4 Linear Displacement Sensors

There are many sensors that can be used to measure stresses, or displacements, of a material. Some common sensors include strain gauges, Hall Effect sensors, and stretch sensors. Strain gauges are widely used to measure the mechanical change in length of a material (Liu & Yang, 2016). The gauge features a thin wire that is organized in grid pattern and outputs an electrical resistance that is proportional to the amount of strain in the material (National Instruments, 2019). This configuration can be seen in Figure 6, above.

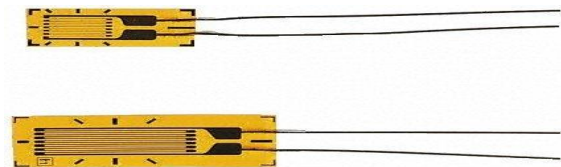


Figure 6. Strain Gauge (Culler, 2017)



Figure 7. Hall Effect Sensor (Core Electronics, 2013)

Strain gauges need to be applied directly onto the material that it is measuring. This usually calls for it to be glued, making it useful for only one material, and unable to be interchangeable. This is disadvantageous because these sensors are relatively expensive.

The second type of sensor, the Hall Effect sensor, uses a magnet to activate it (Electronics Tutorials, 2019). The sensor outputs a voltage that is proportional to the change in distance from the magnet to the sensor, Figure 7. Typical benefits of using this type of sensor include its long life and low cost, although it becomes slightly inaccurate if the magnet is not directly perpendicular to the sensor (Honeywell, 2019).

The last sensor, a stretch sensor, also outputs a resistance like a strain gauge. Stretch sensors use a conductive rubber material that when placed between two alligator clips can measure the change in length due to the particles getting further apart. The rubber resembles a typical black cord, Figure 8, but consists of carbon-black rubber. The readings from a stretch sensor may be slightly inaccurate, but it is useful in measuring stretching motions and is low in cost, like a Hall Effect sensor (Adafruit, 2018).



Figure 8. Stretch Sensor (Sector67, 2019)

2.5 Hydro Muscles

Hydro Muscles are a type of hydraulically, or pneumatically, actuated muscles that resemble biological muscle. They were developed by Professor Marko Popovic in 2014 to allow for a more comfortable user interface with exoskeletons as opposed to the use of a rigid exoskeleton or a rigid-link manipulator (McCarthy et al., 2014). Hydro Muscles expand and contract linearly when they are pressurized and depressurized. They elongate axially and become stiff without allowing for radial expansion. When they contract they become soft radially. The elongation and contraction of the muscle is shown in Figure 9 below.

Relaxed



Pressurized



Figure 9. Hydro Muscle Relaxed and Pressurized (Curran, Colpritt, Sullivan, & Moffat, 2018)

Hydro Muscles are typically used to apply a pulling force much like biological muscles. This is similar to the more popular artificial muscles, McKibben muscles. McKibben muscles become stiff when they are contracted and soften when elongated. These muscles expand radially while contracting axially, therefore they lose a substantial amount of energy.

Hydro Muscles consist of an outer sheathing that is soft and inelastic, typically polyester is used for this outer layer. The polyester allows axial expansion but limits radial expansion, which increases the efficiency and exceeds that of McKibben muscles. The inner portion of the muscle is a smooth, elastic tube such as latex. The tube has two caps at each end, one of which is a valve

for the pressure source. These materials are low in cost making Hydro Muscles cost-effective as well as simple to create.

They are activated by pressurizing them with either air or water. Ordinary tap water can be used at a pressure of 0.59 MPa. Another option is to use compressed air at approximately 100 psi (Sridar et al., 2016). Unlike other wearable exo-musculatures that need a large number of independently controllable units, Hydro Muscles can be actuated using one source to drive multiple muscles (McCarthy et al., 2014).

Applications of Hydro Muscles include uses for orthotic or exoskeletal systems. Some of these systems include elbow or knee exo-musculatures which will allow the user to exert more force that may be needed for physical therapy, daily assistance, or an augmentation system. Another system is a flapping wing system, where a Hydro Muscle mimics the pectoral muscle making a down flap motion when it depressurizes (Sridar et al., 2016). Most recently, Hydro Muscles were used to create a humanoid walking robot in which the muscles were attached to an artificial skeleton in place of biological muscles. The robot successfully demonstrated a walking gait cycle which sets the stage for clinical applications, prosthetics, military defense, or other applications (Curran et al., 2018).

Chapter 3: Project Objectives

This project aimed to gain a better understanding of pitching biomechanics and the stresses endured by the UCL in an overhead throw. This was done by creating a testing mechanism, using Hydro Muscles to actuate a human-like fastball baseball pitch, in which stress measurements were taken on. With more knowledge about the stresses in the UCL, a way to prevent future UCL injuries was developed.

To prevent UCL injuries, the goal of this project was to design a brace that will reduce the amount of valgus torque the arm undergoes during a pitch, and therefore reduce the amount of stress going through the UCL. The testing mechanism mentioned above was used to validate the braces effect.

The objectives for this project are outlined below:

1. Build a model that mimics the movement of a fastball baseball pitch using a skeletal frame with the following biomimetic features:
 - a. Hydro Muscles, replacing the essential muscles in the arm and shoulder.
 - b. An artificial Ulnar Collateral Ligament (UCL), resembling the material properties of a biological UCL.
2. Use the skeletal model to identify and measure the phases in which there were significant spikes in the stress on the artificial UCL throughout the pitch.
3. Build a device that can help prevent UCL tears in amateur and/or professional athletes.
 - . The device will decrease the stress on the UCL without inhibiting the athlete's performance, potentially prolonging play time without injury.
4. Test effectiveness of device using the skeletal model.
 - . The throwing motion with the brace should be the same as without it.
 - a. Force on the UCL should be less with the brace than without.

Chapter 4: Methodology

4.1 Skeletal Model

4.1.1 Hydro Muscles

The Hydro Muscles were used to produce the movement of the skeletal arm model. They are created by using latex tubing, polyester sheathing, various barbed plugs, clamps, and fishing line. Figure 10 shows the components of the Hydro Muscles.

The latex tubing had a 1/2" OD and 1/4" ID, the polyester sheathing fit closely over the tubing, and the barbed plugs were glued at the ends of the tube, using Gorilla glue. Lastly, the clamps were tightened near the ends of the Hydro Muscles and fishing line was tied at the ends of the plugs to attach them to the skeletal arm.



Figure 10. Hydromuscle Materials and Construction (Curran et al., 2018)

The steps listed below detail how to construct a Hydro Muscle:

1. Cut the latex tubing to the desired length. Be sure to make this a clean, flat cut otherwise angled cuts may cause leakages.
2. Cut the polyester sheathing 1/4" longer than the latex tubing.
3. Insert the latex tubing into the sheathing.
4. Slide the worm clamps on both ends of the tubing.
5. Insert the barbed hose fitting on one end partially. Coat the end of the fitting with Gorilla glue before inserting it completely.
6. Insert the barbed plug on the other end partially. Coat the end of the plug with Gorilla glue before inserting it completely.
7. Tighten the clamps as tightly as possible. Be sure to position the clamps so that they are around the portion of tubing where the fitting or plug is inserted.
8. Coat the ends of the polyester sheathing with clear nail polish to prevent fraying.
9. Use a needle to create two small holes at the top surface of the barbed plug. Thread the fishing line through the holes to create a loop in order for the Hydro Muscles to be attached to the model.

In order to determine the initial muscle lengths, the desired change in length were measured. To find this, a string was attached at the insertion point for a specific muscle and fed through an eye hook at its origin. The skeletal arm was then moved to its angle of flexion where an initial mark was made on the string. Then the arm was rearranged to its angle of extension where a mark was made to the final location of the string. The distance between each of the marks on the string were measured as it represents the change in length the Hydro Muscle must achieve. This procedure was repeated for each of the selected muscles. A linear regression was created to determine the relationship between the original length of the latex tube and its change in length, Appendix A.

The muscles were chosen based off of mechanisms of action to keep the model simple enough to feasibly build. Therefore, a total of seven muscles in the shoulder and upper arm were mimicked. These muscles were the teres minor, infraspinatus, triceps brachii, middle deltoid,

biceps brachii, subscapularis, and pectoralis major. The teres minor provided lateral rotation, the infraspinatus provided horizontal abduction, the triceps extension of the elbow joint, the deltoid abduction of the shoulder joint, the biceps flexion of the elbow joint, the subscapularis medial rotation, and the pectoralis horizontal adduction.

4.1.2 Skeleton

Orthopedic surgery training bones were used to resemble a human right arm. These bones were held together in such a way that they could articulate in the same way as a human arm. In the case of the elbow joint, each major ligament bundle was simulated using leather. This was because leather has similar elastic properties to that of a human ligament, which would allow a similar mechanical change. Eye hooks were inserted at the point of insertion and origin for each muscle, allowing an easy Hydro Muscle attachment and guided movement.

3D printed plastic rings were attached to the model to mimic the arm's bulk. These were printed using PLA and included 4 hexagonal shapes removed in uniform spacing around the inside of the ring. These holes were sized so that a standard nut could be pasted in the void, which would accept a threaded rod. The rings themselves were sized to simulate the circumference of an example arm at 4 different locations along the arm. These provided a framework for which a brace could be placed over to simulate the structure of the arm. The 4 rods were tightened to attach the rings to the arm and the excess material was removed, to keep the rods flush with the outer surface of the rings.

4.1.3 Structure

The arm assembly, specifically the scapula, was attached to a 10 inch wide board, which was used to support the Hydro Muscles. The board was attached to a metal frame using hinges, and a control board, with plastic tubing and electrical equipment, sat on top of the metal frame. The metal frame consisted of 80/20 T-slotted aluminum, and the control board was composed of 8 solenoid valves connected to a central air supply and an Arduino.

In order to simulate the twisting of a pitcher's torso during the throw, the base of the board was attached to a protrusion in the metal frame with springs of a spring constant $.4605\text{N/m}$. This and a gate catch on the posterior support, allowed the arm assembly to twist synchronous with the more classical throwing motion of the arm. The gate catch was controlled with another Hydro Muscle in order to simplify the overall system.

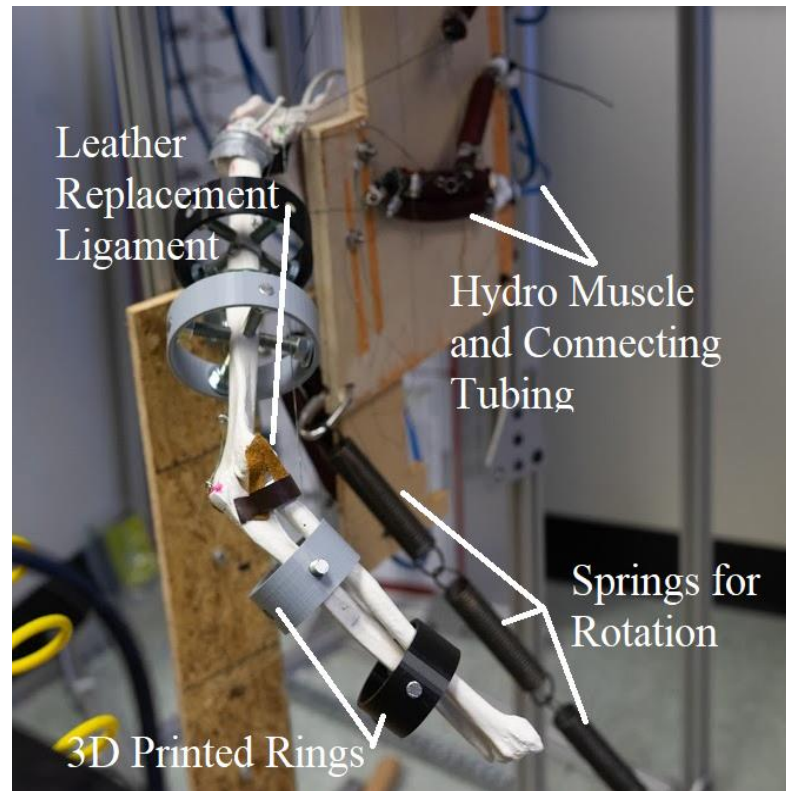


Figure 11. Arm Model Assembly

4.1.4 Air Tank and Valves

In order for the Hydro Muscles to be activated pneumatically, a compressed air tank was used. Although this air tank is capable of supplying compressed air of up to 150 psi, it was operated it at 100 psi to ensure the muscles would not burst. Eight 5-to-2 way Solenoid valves that served as a connection between the air pump and electronic controllers. The solenoid valves were supplied with 0.2 amperes per valve and 24 volts collectively. 5-to-2 way means that the valves have five ports and two flow positions. One port is the air inlet to supply pressure, two of the ports allow air to be regulated when air is flowing out, and two ports power the system. The two flow positions of the valves are either on or off, meaning air is being supplied to or cut off from the muscles (US Solid, 2018). The valves also had a flow control valve connected to them which regulated the flow of the air coming out of the hose side of the valve. These controlled the speed at which the muscles contracted. The air tank, solenoid valves, and muscles were all attached using 1/4" diameter pneumatic tubing and push connects. Single and branched push connects were used to double-up some of the muscles in order for them to exert more force.

4.2 Sensor and Controls

4.2.1 Sensors

Various sensors were considered to measure the stress on the UCL, including Hall Effect sensors, strain gauges, and stretch sensors. The movement of the mechanism presents many challenges in using hall-effect sensors as it is not a linear movement. Strain gauge sensors are

expensive and the attachment to the mechanism impacts the reading from the testing. Stretch sensors, also known as conductive rubber, were chosen as the most convenient for the project's dynamics and its economic cost. This sensor measures stretch forces, when stretched the resistance of the conductive rubber changes (Adafruit, 2018). Due to the fact that the expected displacement/stretch is significantly small, it was decided to combine the stretch sensor with the leather used as the biomimetic UCL, Figure 12. By doing so the sensor will be limited to stretch when the leather is being stretched, there for being closer to the real UCL anatomic motion. Small

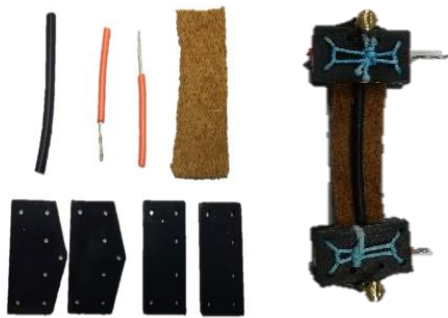


Figure 12. Sensor Materials and Stretch Sensor Configuration

3D printed plates were designed to build the right sensor connections. On the place a point of the leather was glued. Then the stretch sensor was also glued to the leather and a cable was modified to fit next to the leather's end while keeping a connection with the rubber. This will allow accessibility to the voltage reading of the rubber. Another plate was glued on top to guard exposed wires and secure the sensor mechanism together. With this mechanism it's aimed to measure the resistance levels during the pitch motion with and without the brace. The lower the resistance corresponds to high force as the rubber is being stretched due to the force. The higher the resistance the lesser the force.

4.2.2 Arduino Mega

An Arduino Mega was used for the electronic controller of the solenoid valves. The board used was the Arduino MEGA 2560 which featured 54 digital I/O pins and was connected to a computer with a USB cord. This was more than suitable for the application since each of the 8 valves required its own digital pin. Arduino was also used to receive information from the stretch sensor. Two codes were written in the program to synchronize the firing of each of the muscles individually, and start/stop the recording of data from the sensor and export the data to a comma-separated values (CSV) file (Appendix B; Appendix C).

4.3 Brace Design

Two braces designs were chosen to mitigate the forces on the UCL in different ways. The first used passive tension, from strips of elastic, integrated into a soft sleeve, secured distally and proximally with nylon straps. This idea came about by consulting with the WPI Athletic trainers who have degrees in physiology and are experts in treating motion restriction in sports. They suggested having a compressive brace that has some form of elastic feature. Therefore, the idea came about to use strips of elastic that run across the UCL. One of the bands would run from the outer side of the upper arm across the UCL to the back of the forearm. The second band should run opposite, from the inside of the forearm across the UCL to the top of the bicep. The strips of elastic would form an "x" pattern across the UCL over a soft sleeve. This was designed to take part of the load from the UCL and instead have it run through the elastic bands. These bands, for ease of use across different sizes could be easily adjustable since different throwers have different size arms.

The second design used rigid components to eliminate all but the single primary degree of freedom of the elbow joint. This design included a rigid single-articulated bar placed on the

posterior side of the arm. This was contained within a neoprene sleeve which was secured with velcro down the length of it and with a proximal and a distal nylon strap. This brace would force the lower arm to maintain the varus/valgus positioning of the humerus, greatly reducing, if not fully eliminating, the valgus stress in the elbow joint and the major force on the UCL.

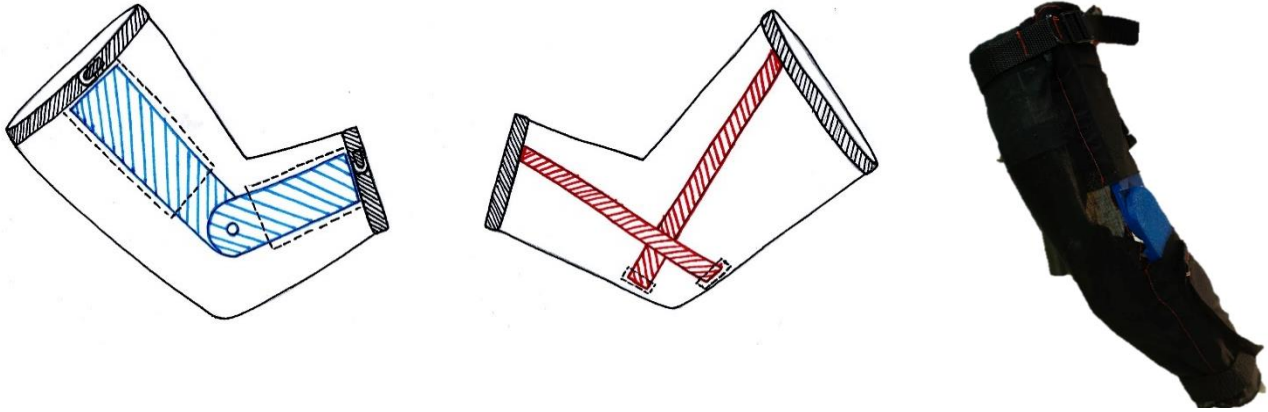


Figure 13. Brace Concepts and Final Prototype

Chapter 5: Experiments

The following chapter details the tests that were performed in order to replicate a human-like baseball pitch in the robotic arm. Many trials of this arm motion were also executed to collect accurate sensor displacement data, with and without the designed brace.

Before data collection began, it was necessary to ensure the motion of the arm resembled that of a fastball baseball pitch. This required the Arduino program to run multiple times while examining the outputted motion of the arm. As described in the methodology, the 8 Solenoid valves were supplied with 100 psi from an air tank, 19 volts from a voltage amplifier, 5 volts from the computer operating the Arduino code, and 1.6 amps. Since the muscles could not be attached to the skeleton when they were contracted, once the current was turned on, all the muscles were expanded to allow origins to be attached easily. To ensure the delays and activation of the muscles in the code were correct, the motion of the skeletal was arm without any masses on it was tested. This helped refine certain aspects that would cause the model to not move in the correct way. Adjustments to the code as well as to the physical model had to be made when the desired motion was not reached. Some of these adjustments included activating certain muscles at different times, changing the length of the fishing line that connected the Hydro Muscles to the bones, or modifying the connection of the shoulder joint. Once the motion without any masses was correct, 3D printed rings were added to the model as base surfaces for testing the brace. Similar modifications, as the ones mentioned previously, had to be made to revert to the acceptable motion. More Hydro Muscles were created to account for the extra mass, from the rings, that needed to be moved and change the direction that some of the muscles would be pulling. This created the correct pitching motion, ready to begin collecting displacement data from the sensor.

Multiple iterations of testing were performed to receive data on the behavior of the UCL during the baseball pitch. During each of these tests, a button is pressed to activate the firing of the muscles, causing the arm to move, and begin data collection from the sensor. The attached stretch sensor delivered data to the Arduino where it was then exported to excel. A total of 24 tests were run to ensure accurate and consistent data was being collected. These tests conducted alternated between iterations without the brace attached to the arm and tests with the brace applied. The data collected from both types of tests were then compared to see if there was a difference in resistance, and thus length change, between the application of the brace, versus without it.

After approximately 5 tests of each with and without the brace, the sensor was removed and calibrated. This was done by hanging the sensor by one end from the frame of the arm model, starting the data recording, and then hanging known masses from the other end. The data was recorded using the same code as used in the throwing tests. The masses were hung in increments of $\frac{1}{2}$ lbs with the change in resistance being recorded to determine a relationship between resistance and force.

Chapter 6: Results

6.1 Comparison of Human and Robotic Arm Pitch

In order to move forward with the force-sensing tests, ensuring that the model was moving accurately was needed. This section compares the motion of the robotic arm, with that of a subject pitcher, as well as videos of professional pitchers. The time lapsed during the throw of the robot and a professional pitcher were considered.

The arm path between the control pitcher and the robotic arm draw to be very similar. Both the test pitcher and the robotic arm started out with an early cocking elbow angle of roughly 33 degrees. These angles were approximated using the Hudl Technique application as seen below.



Figure 14. Early Cocking of Test Pitcher

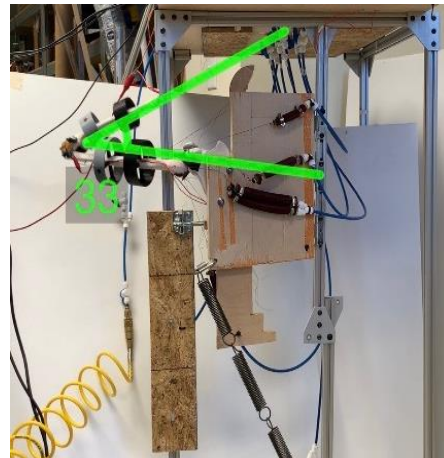


Figure 15. Early Cocking of Robot

As the elbow rapidly accelerated forward, the control pitcher reached an elbow angle just past 150 degrees at which the ball began to roll off the fingers. This would be considered the release point in the throwing motion, as the arm is reaching maximum extension and is created with a 56 degree angle of separation from the core axis to fingertip. The robotic arm was able to create a similar angle which was determined to be its release point, just past 150 degrees, and is met with a 70 degree angle of separation from the core axis.

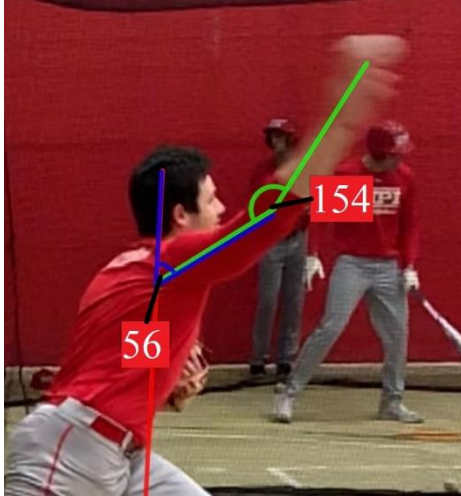


Figure 16. Release Point of Test Pitcher

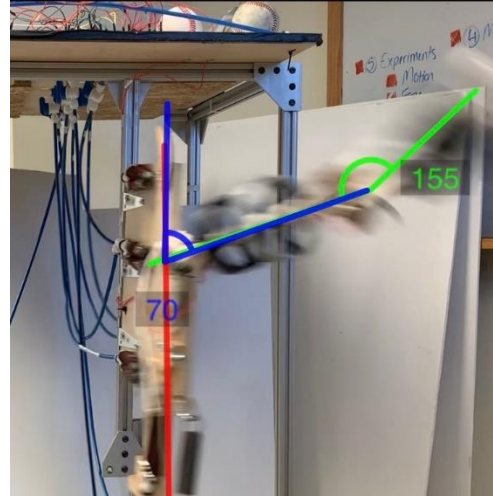


Figure 17. Release Point of Robot

Based on video analysis, a pitcher's trunk will rotate approximately 110 degrees around the z axis. This will occur in about .5 seconds, resulting in a rotation speed of approximately 220 degrees/second (Drysdale, 2012). The arm itself rotated about 100 degrees in .5 seconds, reaching a speed of 200 degrees/second.

6.2 UCL Forces with and without the Brace

In this section, readings from the stretch sensor are reported. The sensor was used to measure the displacement of the synthetic UCL which was associated with the force the UCL experienced. The relationship between force and the outputted resistance from the sensor are also displayed in this section.

As mentioned in Chapter 5, Experiments, the mechanism was tested with and without the brace 24 times each, 8 were not considered due to inaccuracy and noise of the reading, 4 were inconclusive and 12 were considered acceptable results. Readings were only considered when the sensor ended with +/- 1 ohm from its starting resistance.

After 12 acceptable tests without the brace, it was found that on average the stretch sensor changed by -5.588 Ohms when the brace was not applied. The change in resistance peaked during the early cocking, acceleration, and deceleration stages of the throws. When the sensor was calibrated, the addition of ½ lbs of force changed the resistance of the sensor approximately -2.04 Ohms each time. The trendline from this data resulted in the following equation:

$$F(R) = -1.05R - 0.116$$

This relationship, when applied to the tests, resulted in a peak force of 1.07 lbs (4.957 N). The graphs for these two experiments can be seen in Figures 18 and 19.

After 12 acceptable tests with the brace were performed, the stretch sensor showed an average maximum change of -2.399 Ohms when the brace was applied. The resistance change peaked during the early cocking and acceleration stages of the throws. This showed a similar pattern to the resistance change of the tests without the brace. Utilizing the sensor calibration, the peak force was found to be 0.382 lbs (1.922 N). This showed a 61.23% reduction in peak force on the UCL when the brace was applied to the arm, shown in Figure 20.

Resistance Change

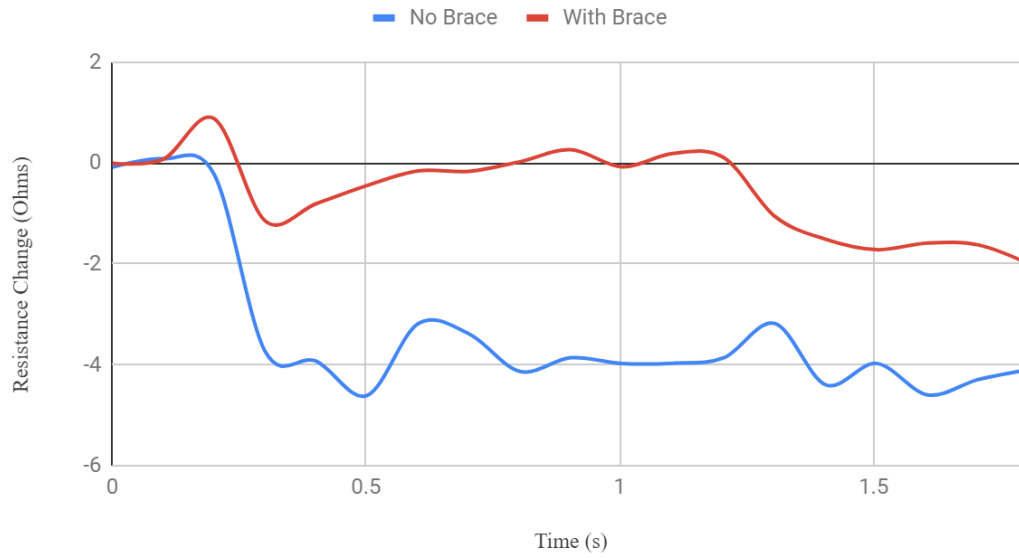


Figure 18. Change in Resistance Through Time Graph

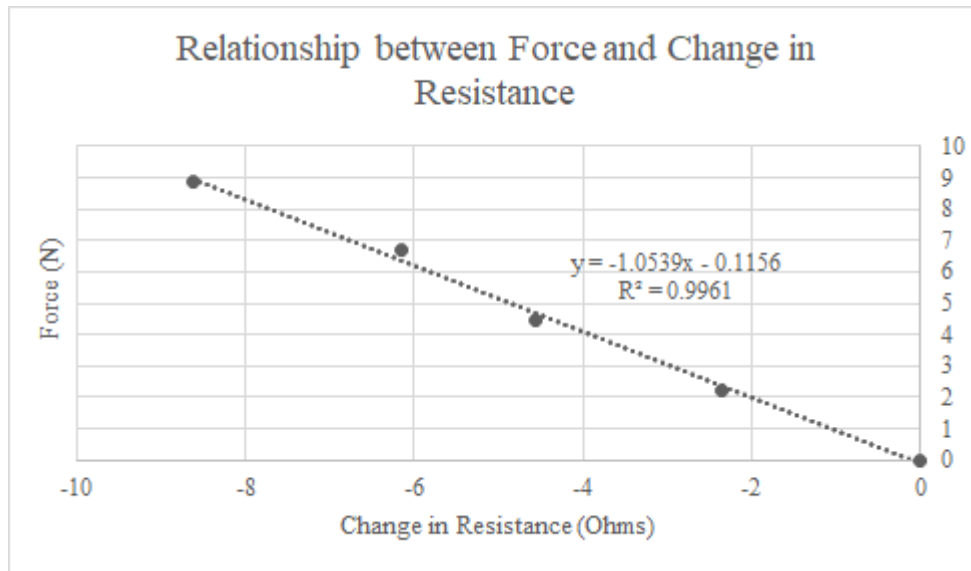


Figure 19. Relationship between Force and Change in Resistance Graph

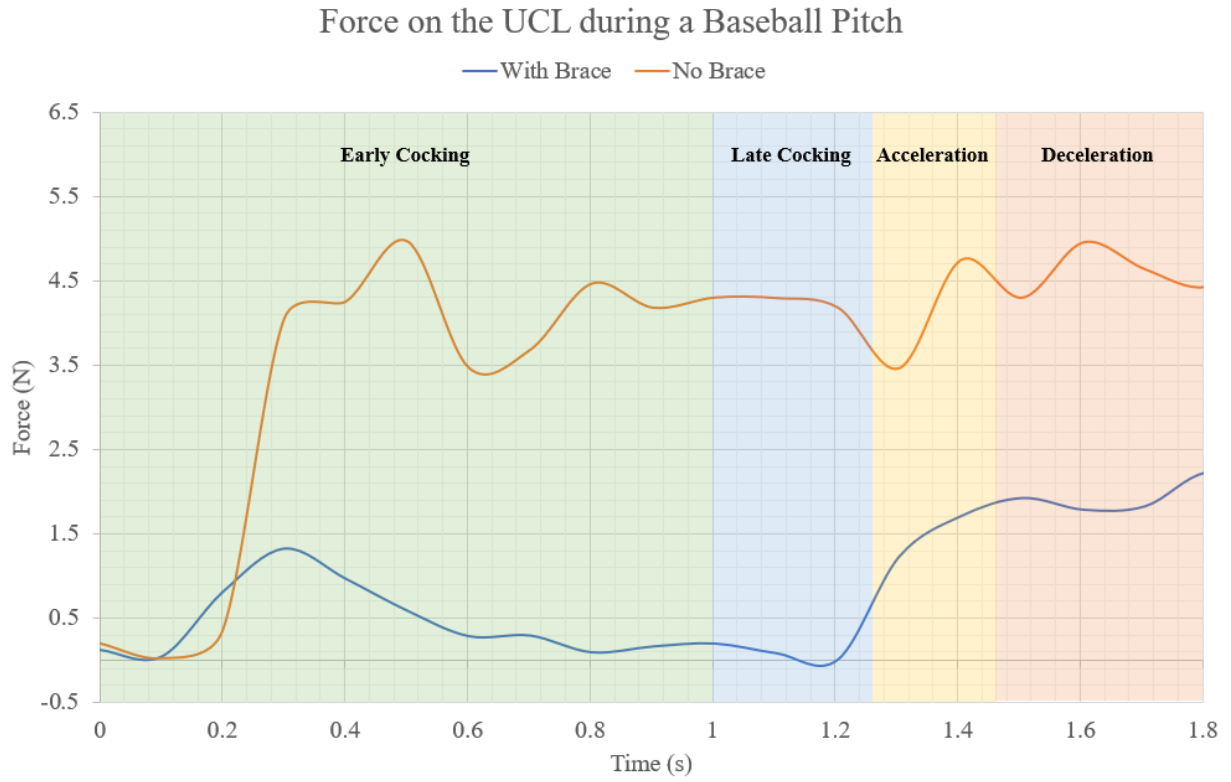


Figure 20. Force on the UCL During a Baseball Pitch Graph

Chapter 7: Discussion

7.1 Analysis of Robot Kinematics

The pitching motion is a complex and fast movement that can be divided into six phases; windup, early cocking, late cocking, acceleration, deceleration, and follow-through. During the early cocking phase, Figure 14 and 15, the smaller preloaded angle allows a higher rotational velocity through the pitching motion as the elbow moves towards full extension, upon, and through release. This would be considered the release point in the throwing motion, as the arm reaches maximum extension. At this point there was a 70 degree core axis angle of the model compared to that of the test pitcher's 56 degree angle. While this difference of roughly 14 degrees may seem alarming, in terms of an average pitcher it would be completely normal since pitching angles often vary in individuals. Pitchers also may experience a humeral drop that can occur mid-outing due to an onset of shoulder fatigue from a large amount of repetitions. Having a smaller angle would also be better for the research because when the elbow drops below 90 degrees at the shoulder joint, a higher stress is created in the elbow during the pitch. Finding not only the phase at which the force is greatest, but also the humeral angle. Therefore, at its initial cocking phase, through its release, the robotic arm angles were relatively close to the pitching angles of the control pitcher which rendered the most accurate results.

This arm was not without its limitations though. First, the model used in this test did not use every muscle in the arm. In order to keep the model manageable, only 6 muscles were used; one for each direction of the desired degrees of freedom. This only allowed a portion of the muscles in the shoulder and arm to impact the motion. Another limitation was that in the body itself, the scapula moves across the ribcage, increasing the horizontal abduction of the shoulder joint. The arm bones used were attached to the pivoting board by bolting it through the scapula which restricted it from fully mimicking natural motion. The arm itself also did not have the correct mass as a biological arm, nor did it have the mass of the hand and ball at the distal end. The incorrect masses meant that, though the timing of the peak forces may be accurate, the numeric values are not the same as the actual force going through a pitcher's arm. The mass was reduced because the pneumatic Hydro Muscles from the current model were not strong enough to maintain the correct motion with additional weight. The last limitation of the model was the valves. Because the valves only had two-states, on or off, the speed of the muscle actuation could not be controlled throughout the pitch and was the same speed for the whole test. The pitching motion requires a slow wind up and then a fast actuation of the muscles, therefore the muscles had to move quickly for the whole test to reach the desired throwing speed. This caused the initial cocking motion of the arm to be exaggerated and jerky.

7.2 Analysis of the Brace's Impact

The data gathered from the stretch sensor during the throwing tests were able to reveal information about the throw. In addition, several shortcomings of the sensor and brace were discovered. These limitations could result in the data to not be as accurate as they could have been.

The force on the UCL was reduced by 61.23% with the application of the brace. This implies that use of the brace could prevent injury to the UCL or increase the number of pitches one executes before injury. This brace was not tested on a human pitcher to ensure that the throw would be unimpeded, but was tested with everyday movements, Figure 21, displaying no

noticeable impediment to movements. This was the only brace tested on the arm model, as the first design was found to not provide adequate support when it was produced. The elastic bands only provided tension on the fabric, simply pulling the fabric up and down the arm without supporting the arm itself.



Figure 21. Brace Prototype Being Worn

The sensor faced limitations as after prolonged periods of tension, the stretch sensor would not retract to its original state immediately. This caused for later readings to be potentially inaccurate. Therefore, tests were only considered if the stretch sensor was able to start and end at the same resistance. This sensor was utilized because the change in length of the UCL was expected to be larger than what a strain gage would be able to handle. The cost of both sensors also directed us to the use of a stretch sensor over a strain gage.

The base material of the brace could also benefit from a change. Neoprene has enough stretch to conform to the arm and provides a padding layer between the hard shank and the arm, but it is not very breathable and has a tendency to tear if stretched too far. Due to these limitations, the brace had to be sized for its specific application, in this case for the arm. This prevented the brace from being tested on a pitcher as the pitcher's arm dimensions did not match those of the model. A more breathable material is also essential for use by pitchers as they are very particular about putting anything on their pitching arm and comfort is essential in order for anyone to actually want to use the brace.

Chapter 8: Conclusion

This project was aimed to create a brace to reduce UCL tears in baseball pitchers since it is one of the most common injuries in these players. This was tested using a mechanical, biomimetic arm model that would move in a similar way to a baseball pitcher. The arm also was used to determine when, during the pitch, the UCL reached its maximum force. A skeletal system was created which featured Hydro Muscles, a spring-loaded hinge, and a synthetic UCL. The Hydro Muscles replicated 3 antagonistic pairs in the upper arm and shoulder and caused the skeletal arm to move. The spring system rotated the skeletal arm which simulated trunk rotation of the body. Lastly, the synthetic UCL was created using leather and attached to the arm in an anatomically correct orientation. Both the Hydro Muscles and the hinge were controlled by eight 5-to-2 way Solenoid valves which were connected to an Arduino board. The Arduino was also connected to a sensor which was attached on the synthetic UCL. This sensor took measurements of the displacement of the material which was then used to find the force going through the artificial UCL.

A brace was then designed to specifically target support for the UCL. Tests without the brace yielded a peak in the force during the acceleration stage of the pitch. When compared to tests with the brace, the force was reduced by 61.23%, while still seeing peaks at the same stages. These results, though informative, could be improved with changes to the brace, sensor, and model.

Features of the brace that could be improved include the 3D printed joint and the base material. A different connection point, such as a bearing, could be implemented for the brace joint to decrease friction and allow for better elbow extension and flexion. Further research on a more elastic, breathable base material for the brace should be done. Durability, comfort, and compatibility between users and the brace could benefit from this newer information. If economically possible, the use of a different sensor, such as a strain gage, should be considered to increase accuracy of the results. Lastly, for the arm model, introducing more muscles in the shoulder, upper arm, and torso could result in a more accurate test. Articulating the scapula to allow for greater horizontal abduction could also yield more realistic results. The addition of more muscle or the replacement of the pneumatic Hydro Muscles to the hydraulic version could increase the strength of the model. This would allow the model to pitch faster, which would better match the speed of a throw, or hold more weight. The weight of the arm could be simulated by using masses at anatomically correct locations, specified in anthropometric charts, and by attaching a baseball to the distal end. The jerking of the arm could be improved by utilizing a dynamic flow-rate control valve, allowing for both slow and fast muscle actuation of the same muscle in the same test. To further artificially mimic the human body, further research using sources, such as *Biomechatronics* by Marko Popovic, would be worthwhile to gain a better understanding of all features of the body. *Biomechatronics* provides recent developments in artificial tissues, prosthetic limbs, natural and synthetic actuators, and control systems that would enable our model to more closely resemble human attributes (Popovic, 2019).

References

- AAU Baseball. (2019). AAU baseball. Retrieved from <https://www.playaaubaseball.com/page/show/1414139-home>
- Adafruit. (2018). Conductive rubber cord stretch sensor + extras. Retrieved from <https://www.adafruit.com/product/519>
- Andrews, J. R., Dugas, J. R., Cain, E. L. & Jost, P. W. (2012). Elbow injuries in the throwing athlete. Retrieved from <https://orthoinfo.aaos.org/en/diseases--conditions/elbow-injuries-in-the-throwing-athlete>
- Bauerfeind. (2016). Sports elbow brace. Retrieved from https://www.bauerfeind.com/b2c/Sports-Brace/Sports-Elbow-Brace/p/YPBF_BAE_EPITRPOWG
- Core Electronics. (2013). A3213 hall effect sensor. Retrieved from <https://core-electronics.com.au/a3213-hall-effect-sensor.html>
- Culler. (2017). Culler strain gauge used in mechanics experiment for material, industry or science (2). Retrieved from <https://www.amazon.com/Mechanics-Experiment-Material-Industry-Science/dp/B01FUNXN0K>
- Curran, A., Colpritt, K., Sullivan, M., & Moffat, S. M. (2018). *Humanoid walking robot* Worcester Polytechnic Institute.
- Dolan, M., & Drew, T. (2005). Tendons and ligaments., 1-15. Retrieved from <http://www.orthonline.dundee.ac.uk/DLS/Orthopaedics%20Rehabilitation%20Technology/Module%20Group%202/Module%202%20-%20Tissue%20Mechanics/Unit%203%20-%20Tendon%20&%20Ligaments/files/assets/downloads/publication.pdf>
- Doran, N. (2015). Running down the velocity upswing. Retrieved from <https://redlegnation.com/2015/02/19/running-down-the-velocity-upswing/>
- Drysdale, C. (2012). Rockies pitcher eddie butler side view. Retrieved from https://www.youtube.com/watch?v=8_eibzFGLsY

- Electronics Tutorials. (2019). Hall effect sensors. Retrieved from <https://www.electronicstutorials.ws/electromagnetism/hall-effect.html>
- Fleisig, G. S., & Andrews, J. R. (2012). Prevention of elbow injuries in youth baseball pitchers. *Sports Health: A Multidisciplinary Approach*, 4(5), 419-424. doi:10.1177/1941738112454828
- Fusaro, I., Orsini, S., Sforza, T., Rotini, R., & Benedetti, M. G. (2014). The use of braces in the rehabilitation treatment of the post-traumatic elbow. *Joints*, 2(2), 81-86. Retrieved from <https://www.ncbi.nlm.nih.gov/pubmed/25606548> <https://www.ncbi.nlm.nih.gov/pmc/PMC4295667/>
- History Staff. (2019). Who invented baseball. Retrieved from <https://www.history.com/news/who-invented-baseball>
- Honeywell. (2019). *Hall effect sensing and application*. Freeport, Illinois: Honeywell Inc.
- Johns Hopkins Medicine. (2019). Tommy john surgery (ulnar collateral ligament reconstruction). Retrieved from <https://www.hopkinsmedicine.org/health/treatment-tests-and-therapies/tommy-john-surgery-ulnar-collateral-ligament-reconstruction>
- Labott, J. R., Aibinder, W. R., Dines, J. S., & Camp, C. L. (2018). Understanding the medial ulnar collateral ligament of the elbow: Review of native ligament anatomy and function. *World Journal of Orthopedics*, 9(6), 78-84. doi:10.5312/wjo.v9.i6.78
- Liu, L., & Yang, Y. (2016). In Liu L., Yang Y.(Eds.), *6 - case study of a piezoelectric steering platform*. San Diego: Butterworth-Heinemann. doi://doi.org/10.1016/B978-0-12-803528-3.00006-9
- LMH Health. (2019). *Ulnar collateral ligament of the elbow reconstruction* The Lawrence Memorial Hospital dba LMH Health.
- McCarthy, G., Effraimidis, D., Jennings, B., Corso, N., Onal, C. D., & Popovic, M. (2014). Hydraulically actuated muscle (HAM) exo-musculature. Retrieved from <http://users.wpi.edu/~mpopovic/media/pubs/HAMproceedingSubmitted1.pdf>
- McDavid. (2019). Compression arm sleeve/single. Retrieved from <https://www.mcdavidusa.com/compression-arm-sleeve-single>

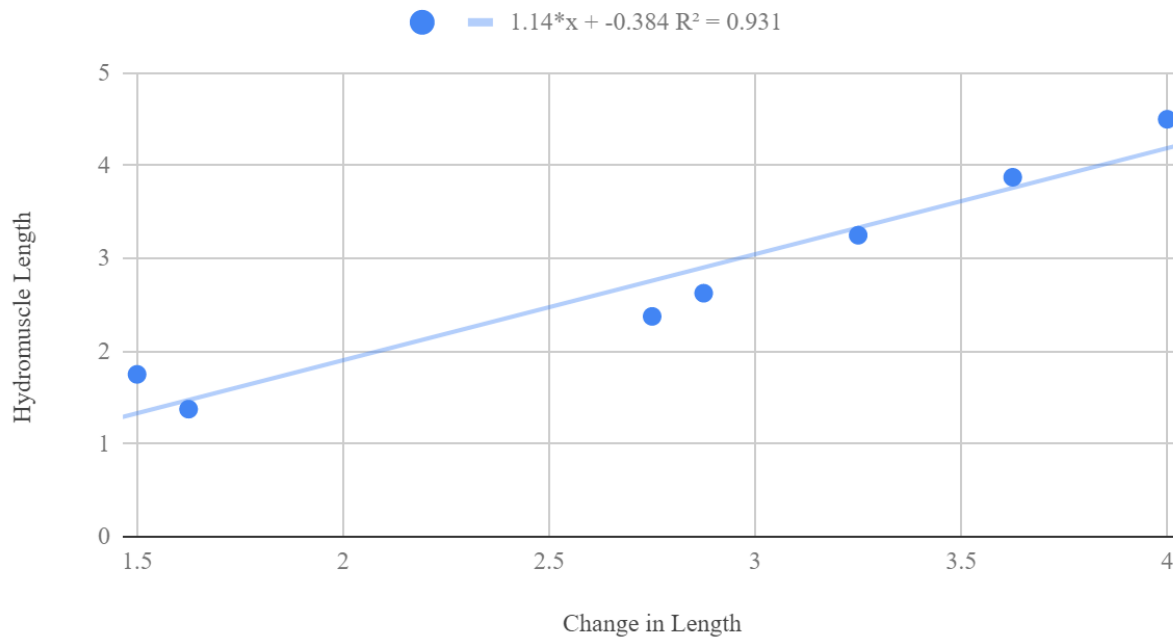
- National Instruments. (2019). Measuring strain with strain gages. Retrieved from <http://www.ni.com/en-us/innovations/white-papers/07/measuring-strain-with-strain-gages.html>
- Ortho Depot. (2019). DLX range of motion post op elbow brace, left. Retrieved from <https://www.fishpond.com.fj/Health/DLX-Range-of-Motion-Post-Op-Elbow-Brace-Left/0610074695769>
- OrthoInfo. (2018). *Baseball injury prevention* American Academy of Orthopaedic Surgeons.
- Oyama, S. (2012). *Baseball pitching kinematics, joint loads, and injury prevention*
doi://doi.org/10.1016/j.jshs.2012.06.004
- Participation statistics. (2013). ().National Federation of State High School Associations. Retrieved from <http://www.nfhs.org/ParticipationStatics/ParticipationStatics.aspx/>
- Perfect Game. (2019). About perfect game. Retrieved from <https://www.perfectgame.org/aboutpg.aspx>
- Physiopedia contributors. (2019). *Throwing biomechanics* Physiopedia.
- Popovic, Marko B. *Biomechatronics*. Academic Press, 2019.
- Sector67. (2019). Conductive rubber cord stretch sensor. Retrieved from <http://www.sector67.org/blog/shop/electronics/conductive-rubber-cord-stretch-sensor/>
- Sridar, S., Majeika, C. J., Schaffer, P., Bowers, M., Ueda, S., Barth, A. J., . . . Popovic, M. (2016). *Hydro muscle -a novel soft fluidic actuator* IEEE. doi:10.1109/ICRA.2016.7487591
- T Seroyer, S., Nho, S., Bach, B., Bush-Joseph, C., P Nicholson, G., & Romeo, A. (2010). *The kinetic chain in overhand pitching: Its potential role for performance enhancement and injury prevention*
doi:10.1177/1941738110362656
- US Solid. (2018). 1/4" 5 way 2 position pneumatic electric solenoid valve DC 24 V. Retrieved from <https://ussolid.com/1-4-5-way-2-position-pneumatic-electric-solenoid-valve-dc-24-v.html>

Appendix A

Hydro Muscle Linear Regression:

Change in Length	Initial Length
1.5	1.75
1.625	1.375
2.75	2.375
2.875	2.625
3.25	3.25
3.625	3.875
4	4.5

Change in Length vs Initial Length



Appendix B

Valve Code:

```
// Pin def
const int buttonPin = 2;
const int subs = 5;    //pin for subscapularis
const int infra = 11; //pin for infraspinatus
const int pect = 9;    //pin for pectoralis
const int teres = 25; //pin for teres minor
const int bicep = 7;   //pin for bicep
const int tricep = 6;  //pin for tricep
const int latch = 28; //pin for latch

void setup() {
  // put your setup code here, to run once:
  Serial.begin(115200);
  pinMode(buttonPin, INPUT); //pin giving feedback
  pinMode(subs, OUTPUT);
  pinMode(infra, OUTPUT);
  pinMode(pect, OUTPUT);
  pinMode(teres, OUTPUT);
  pinMode(bicep, OUTPUT);
  pinMode(tricep, OUTPUT);
  pinMode(latch, OUTPUT);
}

void loop() {          //This is the sequence of performance
  All_Expanded();     //normal state before button is pressed
  if(digitalRead(buttonPin)==HIGH){ //when button is pressed this will be activated
    delay(5000);      //5 seconds before sequence starts
    Early_Cocking();
    All_Expanded();
  }
}

void All_Expanded(){ //command for all muscles to be expanded
  digitalWrite(subs, HIGH);
  digitalWrite(infra, HIGH);
  digitalWrite(pect, HIGH);
  digitalWrite(teres, HIGH);
  digitalWrite(bicep, HIGH);
  digitalWrite(tricep, HIGH);
  digitalWrite(latch, HIGH);
}

void Early_Cocking(){ //command for pitching motion (cocking, late cocking, acceleration)
  digitalWrite(subs, HIGH);
  digitalWrite(infra, LOW);
}
```

```
digitalWrite(pect, HIGH);  
digitalWrite(teres, LOW);  
digitalWrite(bicep, LOW);  
digitalWrite(tricep, LOW);  
digitalWrite(latch, HIGH);  
delay(1000);  
digitalWrite(subs, LOW);  
digitalWrite(infra, HIGH);  
digitalWrite(pect, LOW);  
digitalWrite(teres, HIGH);  
digitalWrite(latch, LOW);  
digitalWrite(bicep, HIGH);  
digitalWrite(tricep, LOW);  
delay(1000);  
}
```


Appendix C

Sensor Code:

```
//Pin def
#define RESISTOR 10000 //This should be the same value of the used resistor
#define Ssensor A0 //This is the pin where the cord is connected tp
unsigned long minutes = 5000;
unsigned long firstTime = 0;
const int buttonPin = 2;
boolean buttonstate=false;
boolean button;

void setup(void) {
  Serial.begin(9600);
  pinMode(buttonPin, INPUT); //pin giving feedback
  Serial.print("Time");
  Serial.print(", ");
  Serial.print("Analog reading");
  Serial.print(", ");
  Serial.print("Voltage");
  Serial.print(", ");
  Serial.println("Resistance");
}

void loop(void) {
  button=digitalRead(buttonPin);
  if (button==true){
    buttonstate=true;
    firstTime = millis();
  }
  if (buttonstate == true){
    Sensor();
  }
}

void Sensor(){
  int value;
  int raw = 0;
  int vin = 5;
  float vout = 0;
  float R1 = 10;
  float R2 = 0;
  float buffer = 0;
  float Force = 0;
  float conductance = 1000000;
  if (millis()-firstTime <minutes*2){
    Serial.print(millis()-firstTime);
    Serial.print(", ");
```

```
value = analogRead(Ssensor); //Read value
Serial.print(value);          //Print value
Serial.print(", ");
vout = value * 5.0 / 1023.0 ;
buffer = (vin / vout)- 1;
R2 = R1 / buffer;
Serial.print(vout);
Serial.print(", ");
Serial.println(R2);
delay(99);
}
else {
void end(void);
button==false;
buttonstate == false;
}
```